Proceedings of Ninth World Conference on Earthquake Engineering
August 2-9, 1988, Tokyo-Kyoto, JAPAN (Vol.V)

7-10-13

STUDY ON THE SEISMIC ISOLATED SPENT FUEL STORAGE RACK

Katsuhisa Fujita[1], Mamoru Tanaka[1]
Masaaki Nakamura[2] and Yonezo Tsujikura[3]

[1]Takasago R&D Center, Mitsubishi Heavy Industries, Ltd.
Takasago, JAPAN
[2]Kobe Shipyard and Engine Works, Mitsubishi Heavy Industries, Ltd.
Kobe, JAPAN
[3]Nuclear Power Operations Department, The Kansai Electric Power Co., Inc.
Osaka, JAPAN

SUMMARY

The present paper aims to evaluate the feasibility of the application of seismic isolation system to a PWR spent fuel storage rack from the view point of the seismic response.

Considering the environmental conditions, two types of isolation systems; sliding type and rolling type are investigated experimentally by a scale model test using a shaking table.

A non-linear seismic response analysis is also performed and it is confirmed that both types of isolation systems investigated are available to the PWR spent fuel storage rack from the view point of the seismic safety.

INTRODUCTION

For increasing the capacity of the spent fuel storage facility, it is effective to decrease the spacing pitch of each fuel assembly in the spent fuel storage rack. At that time, however a difficulty on structural strength arises, that is, increased seismic loads on stored fuel assemblies will require increased strength of the rack itself, and also the wall and the floor of the spent fuel storage pit will be required to have increased strength to support the seismic load on the rack. To avoid such difficulties, the introduction of a seismic isolation system to a PWR spent fuel storage rack is studied.

There are some applications of seismic isolation systems to spent fuel storage racks (Refs.1,2,3), however careful consideration is required to determine the most suitable specification under the restriction of plant manufacturing and construction. Because the seismic isolation systems generally have some non-linearities and especially fluid-structure interaction for a spent fuel storage rack should be accounted in seismic response evaluation (Refs.4,5).

This report describes the results of the shaking table experiment using a reduced scale model and the results of the non-linear seismic response analysis, they are conducted to determine the seismic isolation system for a PWR spent fuel storage rack.

SEISMIC ISOLATION SYSTEM

The seismic isolation system applied to the spent fuel rack must keep its function during the plant life, under the radio activity and hot water condition. Thus, finally following two types of seismic isolation systems shown in Fig. 1 are investigated in this paper.

(1) Sliding isolation system

Seismic load is decreased by a slip between a metal linear installed on the floor of the spent fuel pit, and also the sliding pad attached on the bottom of the rack. Graphite pellets are plugged into the metal pad to decrease the friction coefficient of the sliding isolation system.

(2) Rolling isolation system

Metal blocks having concave surface are installed on the floor and on the bottom of the rack, and a circular cylindrical roller is installed between them. When a horizontal load is applied to the rack, the roller moves along the concave surface and the rack moves horizontally and a little vertically, then the gravitational force acts as a restoring force to the rack. Thus, the rack is considered to be supported by a non-linear spring.

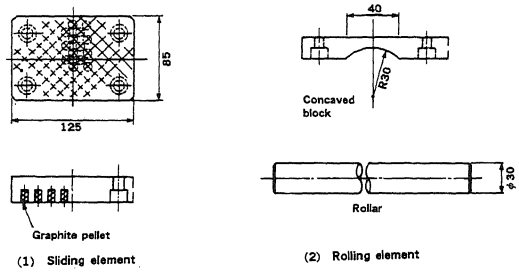

Fig. 1 Seismic Isolation Systems

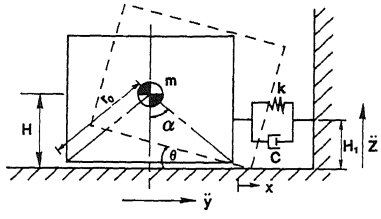

Fig. 2 Analytical Model

SEISMIC RESPONSE ANALYSIS

In the following analysis, the upper structure of the seismic isolated spent fuel storage rack is considered to be rigid, because the stiffness of the upper structure is very stiff comparing with the vibration characteristics of the isolated system itself. In the analytical model shown in Fig. 2, virtual mass and displaced mass of the fluid are considered on the mass of the rack.

The equation of the rack motion in horizontal and rotating (rocking) directions are expressed as follows respectively;

$$(m+m_H)\ddot{x}+c(\dot{x}+\dot{\theta}H_1)+k(x+\theta H_1)+(m-m_D)(g+\ddot{Z})\mu=-(m-m_D)\ddot{y} \tag{1}$$

$$\begin{aligned}&(mr_0^2+m_R)\ddot{\theta}+(m-m_D)(g+\ddot{Z})r_0\sin(\alpha-\theta)+(m+m_H)\ddot{x}r_0\cos(\alpha-\theta)\\&+c(\dot{x}+H_1\dot{\theta})H_1+k(x+H_1\theta)H_1=-(m-m_D)\ddot{y}r_0\cos(\alpha-\theta)\end{aligned} \tag{2}$$

where,

m : mass of the rack
x : horizontal rack displacement (relative to the it floor)
θ : rotational angle
m_H : virtual mass of the fluid for horizontal rack motion
m_R : virtual mass of the fluid for rotational rack motion
m_D : displaced mass of the fluid
c : damping coefficient for horizontal rack motion
k : restoring force for horizontal rack motion

and, $(\dot{x},\ddot{y},\theta)$ denotes the friction coefficient between the rack and the floor and has following values according to the rack motion.

$$(\dot{x},\ddot{y},\theta) = \begin{cases}\mu_{SF}\ \mathrm{sgn}(\ddot{y}) & (\dot{x}=0,\ \theta=0 : \text{stop condition})\\ \mu_{DF}\ \mathrm{sgn}(\dot{x}) & (\dot{x}\neq 0,\ \theta=0 : \text{sliding condition})\\ \mu_{SL}\ \mathrm{sgn}(\ddot{y}) & (\dot{x}=0,\ \theta\neq 0 : \text{rocking condition})\\ \mu_{DL}\ \mathrm{sgn}(\dot{x}) & (\dot{x}=0,\ \theta\neq 0 : \text{sliding and rocking condition})\end{cases} \tag{3}$$

where,

μ_{SF} : static friction coefficient at surface contact
μ_{SF} : dynamic friction coefficient at surface contact
μ_{SL} : static friction coefficient at line contact
μ_{DL} : dynamic friction coefficient at line contact

Thus, in the numerical calculation, the value of μ should be determined in each calculation time step according to the conditions in Eq. (3). The numerical response calculation is performed by the Runge-Kutta-Gill method, and the friction coefficient is determined by Eq. (3).

The other hand, the restoring force of the rolling system is described in the form of a non-linear spring as follows;

$$k(x)=\frac{F}{x}=(m-m_D)\left(\frac{g+\ddot{z}}{\sqrt{1-x^2}}-\frac{\dot{x}^2+x\ddot{x}}{1-x^2}-\frac{x^2\dot{x}^2}{(1-x^2)^2}\right) \tag{4}$$

In the numerical calculation, the value of k(x) is also determined in each time step according to the values of x,$\dot{x}$ and $\ddot{x}$.

SHAKING TABLE EXPERIMENT

A series of shaking table experiments had been conducted using a reduced scale model of a spent fuel storage rack. Since the effect of gravitational accerelation is not able to neglected for the vertical load in the sliding system and the restoring force of the rolling system, and since model and the prototype are located in the same gravitational field, the similarity ratio on the accerelation is settled to 1 : 1 as shown in Table 1.

The test model rack is manufactured by scalling down the design specifications of the prototype rack. The upper structure of the rack is made by steel plate and it can be considered to be approximately rigid in the test condition. The fuel assemblies are assumed to be a dead mass and corresponding additional masses are attached to the rack.

The test was performed using a shaking table driven by a hydraulic actuator, and excited horizontally. The test apparatus is shown in Fig. 3.

The seismic response behavior of the model rack is measured by accelerometers and displacement transducers, and measured signals of the rack motion and the table accerelation signals are recorded in a data recorder. The play back signals are processed by a digital computer.

An artificial earthquake wave (maximum accerelation : 500gal, duration : 33.09 sec.) shown in Fig. 4 is employed for the excitation wave, and according to the similarity law shown in Table 1, time scale is compressed as 1/2.83 for the standard test condition. Moreover, to investigate the seismic response for different input frequency characteristics, the test using the time compression of 4/2.83, 2/2.83 and 0.5/2.83 are also conducted.

The friction coefficient of the sliding isolation system, restoring force of the rolling system and the virtual mass and virtual damping of the fluid are measured to use the simulation analysis. At the measurement of the friction coefficient of the sliding system, forced displacement of a triangular wave form is applied to the model rack and the reaction force is measured. An example of the measured friction force is shown in Fig. 5. Where the sliding velocity is determined from the inclement of the displacement signal along to the time axis and the relationship between the sliding velocity and the friction coefficient is obtained. The result is shown in Fig. 6, and it shows that the friction coefficient is almost constant to the sliding velocity in the tested velocity range. The static friction coefficient is evaluated from the force at the initiation of the slip by increasing the applied force to the rack gradually.

Table 1 Similarity Raw

Physical unit	Symbol	Dimension	Ratio
Length	L	[L]	L_m / L_p (*) = 1/8
Mass	M	[M]	M_m / M_p = 1/512
Time	T	[T]	T_m / T_p = $\sqrt{1/8}$ = 1/2.83
Displacement	δ	[L]	δ_m / δ_p = 1/8
Velocity	v	$[LT^{-1}]$	v_m / v_p = 1/2.83
Accerelation	a	$[LT^{-2}]$	a_m / a_p = 1
Force	F	$[MLT^{-2}]$	F_m / F_p = 1/512
Stress	σ	$[ML^{-1}T^{-2}]$	σ_m / σ_p = 1/8
Frequency	f	$[T^{-1}]$	f_m / f_p = 1/2.83

* Note; Suffix m denotes the model and suffix p denotes the prototype

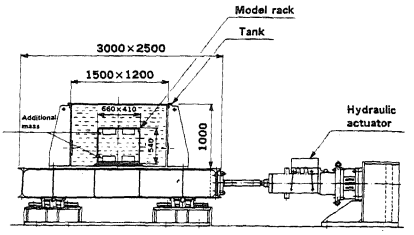

Fig. 3 Experimental Apparatus

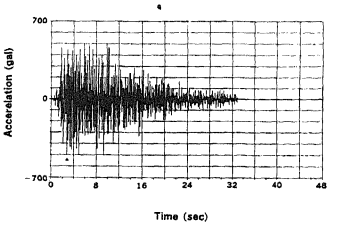

Fig. 4 Input Earthquake Wave

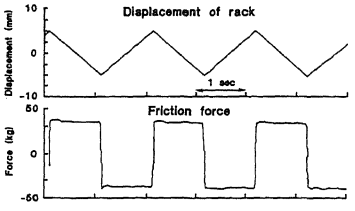

Fig. 5 Time History of Friction Force

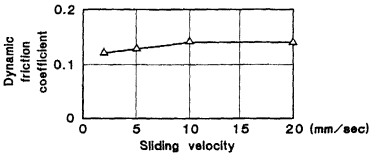

Fig. 6 Friction Coefficient

EXPERIMENTAL RESULTS

On the seismic response of the experimental model, experimental results are compared with calculated results. The measured acceleration signals of the shaking table are converted to digital data and applied to the numerical analysis.

Fig. 7 shows the comparison of measured and calculated seismic response at a typical test condition. The results for the sliding system shows that the displacement response wave is well estimated by the analysis and the stick-slip behavior is well simulated. On the other hand, the results for the sliding system shows that the calculated displacement response rises steeper than measured response and it shows that damping is underestimated in the calculation. The reason is that the analytical model considers only virtual damping of the fluid and the damping due to the friction of the roller is not accountes in the analytical model.

The maximum acceleration and maximum displacement of the rack response are plotted against the maximum acceleration of the shaking table for each isolation system as shown in Fig. 8 and Fig. 9 respectively.

In case of the sliding system, the difference between measured and calculated results in displacement response decreases for the long period input (T=2/2.83 and 4/2.83). The reason is considered that the estimation error of the transient between stick and slip conditions becomes not so significant and the amount of displacement during the slilding condition dominates for the long period input.

On the other hand, the response of rolling system increases remarkably for long period input. The reason is considered that the natural frequency of the rolling system locates 2.5-3Hz, and predominant frequency of the input

approaches to this frequency range in case of long period input. Thus the natural frequency component predominates in the response, and the under estimation of the damping in calculation causes over estimation of the response for long period input.

As mentioned above, it is verified that the presented analysis method simulates the experimental results with reasonable accuracy. And it is found that both types of isolation systems works well for the design condition earthquake. However, for long period and large acceleration input the rolling type isolation system has the possibility to cause a resonance with the low frequency component of the input wave, and the safety margin is limited.

Thus, the sliding type seismic isolation system is most applicable for the PWR spent fuel storage rack.

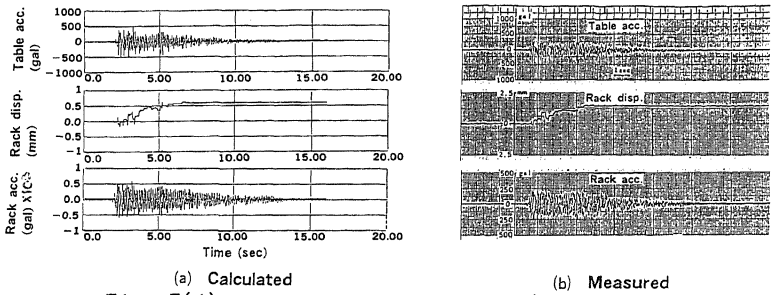

(a) Calculated (b) Measured

Fig. 7(1) Response Time History (Sliding Element)

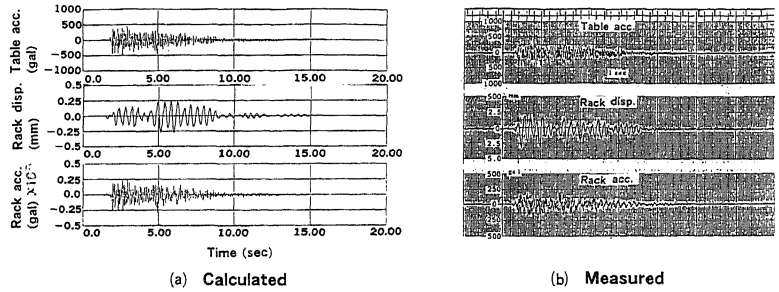

(a) Calculated (b) Measured

Fig. 7(2) Response Time History (Rolling Element)

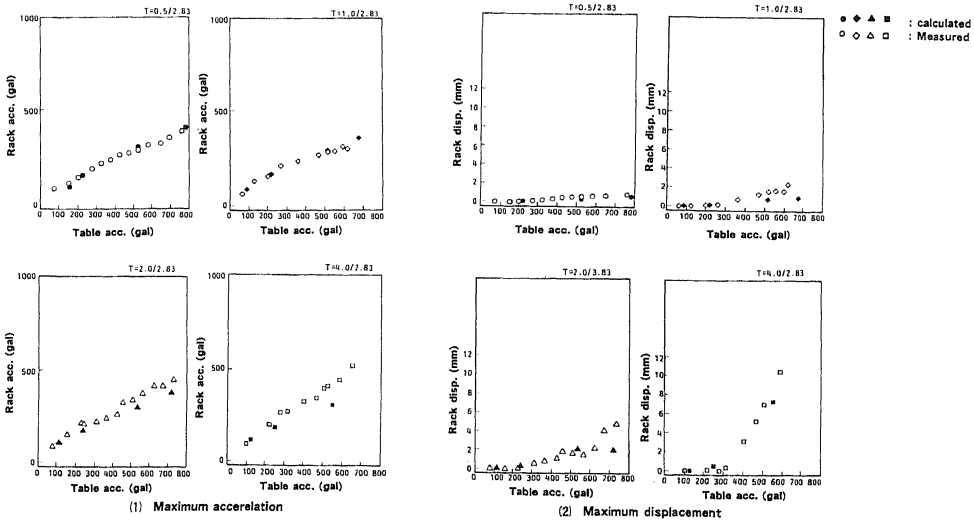

Fig. 8 Maximum Response of Sliding Element

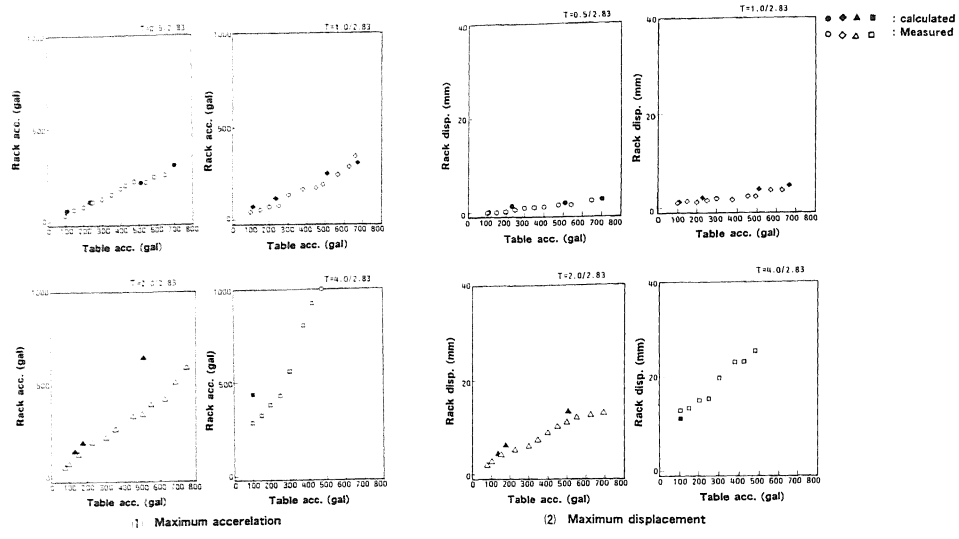

Fig. 9 Maximum Response of Rolling Element

CONCLUSION

A series of model experiments and non-linear seismic response analysis have been conducted to select the seismic isolation system applied to a PWR spent fuel rack, and follwing results are obtained;

(1) The model test results show that both types of seismic isolation systems investigated, that is, sliding type and rolling type have sufficient seismic isolation performance.

(2) The seismic response analysis considering the non-linearities of the isolation systems is proposed, and its propriety is verified by the model experiment.

(3) The sliding type isolation system is most applicable for a PWR spent fuel storage rack, since it has enough safety margin for the long period and high level input earthquake.

ACKNOWLEDGMENTS

Contents of this paper is a part of the results of the cooperative study with following Japanese electric companies; The Kansai Electric Power Co., Inc., Hokkaido Electric Power Co., Inc., Shikoku Electric Power Co., Inc., Kyushu Electric Power Co., Inc., and The Japan Atomic Power Company.

REFERENCES

1. South California Electric & Gas., "Licensing report on High-Density Spent Fuel Racks for Virgil C. Summer Nuclear Station.", NRC Docket No.50-395. (1983).
2. Arkansas Power & Light Co., "Arkansas Nuclear One Units 1 & 2 Additional Information Concerning Spent Fuel Storage Expansion", NRC Docket No.50-313, 50-368. (1983).
3. Portland G.E.Co., "Trojan Nuclear Plant Spent Fuel Storage Rack Replacement Report.", NRC PDR Documents PGE-1073. (1983).
4. Soler, A.I., "Seismic Response of Free Standing Spent Fuel Rack Construction to 3-D Floor Motion.", ASME Paper No.83-NE-10. (1983).
5. Harstead, G.A., "Seismic Analysis of High Density Spent Fuel Storage Racks.", ASME Paper No.83-NE-11. (1983).